Materials. All chemicals used in this research were analytical grade and used as received unless otherwise stated. Potassium carbonate (K_2CO_3), Potassium iodide (KI) and hydrochloric acid (HCl) were obtained from FUJIFILM Wako Pure Chemical Corporation, Japan. 9-chloromethylanthracene, rhodamine 6G, tetrakis(4-carboxyphenyl)porphyrin (TCPP), and rose bengal (RB) were obtained from Tokyo Chemical Industry (TCI), Japan. SOSG was obtained from Thermo Fisher Scientific. Solvents in reagent grade were obtained from FUJIFILM Wako Pure Chemical Corporation, Japan. **rTPA** was synthesized and characterized according to the literature.[1]

Synthesis and Characterization of RA. Rhodamine 6G (1.00 g, 2.08 mmol) and 9-chloromethylanthracene (0.470 g, 2.07 mmol) were dissolved in 300 mL of dry acetonitrile. Then, K_2CO_3 (2.70 g, 19.5 mmol) and KI (1.00 g, 6.0 mmol) were added to the solution, and this reaction mixture was stirred at 65 ^oC for 24h. The reaction mixture was cooled to room temperature and excess water was added and extracted using dichloromethane (4×50 mL). The organic layer was collected and dried over anhydro anhydrous $MgSO_4$, and the solvent was evaporated. The product was purified by silica gel chromatography using a methanol: chloroform mixture (1:20, v/v) as the eluent. **RA** was obtained as a purple powder (100 mg, 8.8 %). *^1H NMR (dimethylsulphoxide-d_6) 500 MHz* δ = 8.67 (s, 1H; Ar-H), 8.45 (br.s, 1H; N-H), 8.40 (d, 2H; Ar-H), 8.29 (d, 1H; Ar-H), 8.14 (d, 2H; Ar-H), 7.95 (dd, 1H; Ar-H), 7.88 (dd, 1H; Ar-H), 7.80 (s, 1H; Ar-H), 7.56 (m, 5H; Ar-H), 7.08 (s, 1H; Ar-H), 6.97 (s, 1H; Ar-H), 6.93 (s, 1H; Ar-H), 5.62 (AB quartet, 2H; N-CH_2-Ar) , 3.98 (m, 2H; N-CH_2), 3.62 (q, 2H; O-CH_2, *J* = 7.0 Hz), 3.05 (m, 2H; N-CH_2), 2.19 (s, 3H; Ar-CH_3), 2.17 (s, 3H; Ar-CH_3), 1.30 (t, 3H; CH_3, *J* = 7.0 Hz), 0.89 (t, 3H; CH_3, *J* = 7.0 Hz). 0.82-0.85 (t, 3H; CH_3, *J* = 7.0 Hz). ESI-Mass: calcd. for $C_{43}H_{40}N_2O_2$: 616.31 m/z, observed: 616.31 m/z.

Electrochemical measurements. Electrochemical measurements were performed using a BAS ALS 630 electrochemical analyzer. Redox potentials were determined by differential pulse voltammetry (DPV) in deaerated dry dimethylformamide (DMF). A glassy carbon (3 mm diameter) working electrode, an Ag/$AgNO_3$ (0.01 M $AgNO_3$) reference electrode, and a Pt wire counter electrode were employed. Ferrocene was used as the internal standard.

Isolation and characterization of the product between 1 and $^1O_2$

3.0 mM **RA** and 3.0 mM TCPP were mixed in 800 μL dry DMF and illuminated by a 430 nm LED light (CL, Asahi-spectra co. Ltd., Japan) for 10 min at 100 mW cm^{-2}. The reaction mixture was subjected to an HPLC system (Agilent 1220) equipped with C18-MS-II column (Nacalai; 4.6 mm I.D. × 250 mm) using DMF as the eluent. Two fractions were obtained and removed the solvent in a vacuum in the dark. The sample was dissolved in DMSO-d_6 and measured the NMR spectra.

Determination of the $^1O_2$ quantum yield. $^1O_2$ was generated using rhodamine 6G, **RA**, and Rose Bengal. A sample solution containing the 2.0 μM of the compound and 10 μM SOSG in 10 mM aqueous HEPES was irradiated by a 532 nm light (20 mW cm^{-2}) for the photosensitized $^1O_2$ generation. The absorption and fluorescence spectra of the samples were measured at regular intervals at 0, 2, 5, 10, 15, and 30 min.

The $^1O_2$ quantum yield was obtained from the following calculations, where the value of Rose Bengal is $\Phi_{\Delta RB} = 0.76$ in water.[2]

$$\emptyset_{\Delta}^{RA} = \frac{r_{RA}}{r_{RB}} \times \frac{C_{RB} \times \varepsilon_{RB}}{C_{RA} \times \varepsilon_{RA}} \times \emptyset_{\Delta}^{RB}$$

Cell culture. PCI-55 was established by our group from pancreatic ductal adenocarcinoma tissues that were resected from primary sites at Hokkaido University Hospital.[3] HeLa cells were obtained from the RIKEN cell bank. HeLa cells and PCI55 cells were cultured in 10% fetal bovine serum (FBS)-Dulbecco's modified Eagle's minimal essential medium (DMEM) with low glucose, additional complement with penicillin and streptomycin. Cells were cultured in a 37 °C incubator with 5% CO_2/air. The cells passages were performed at 90% confluency.

Confocal microscopy imaging. The fluorescence signals of the probe molecules were detected using a High-Speed Laser Confocal Microscope (Nikon-A1Rsi, Nikon Corporation, Tokyo, Japan). The microscope is equipped with an oil-immersion objective lens (Plan Apo VC, 60x, NA 1.4) and a dichroic mirror (DM405/488/561/640). After culturing Hela cells or PCI55 cells on a glass-bottom dish for 1 day, the culture medium mixture was removed and cells were washed with Hanks' Balanced Salt Solution (HBSS(+)). The cells were incubated in the 100 nM MitoTracker™ Deep Red FM (ThermoFischer Scientific, USA) containing medium for 10 min. Then, a 1.0 mM solution of **RA** in DMSO was added to the dish (final concentration of **RA** in the dish: 10 μM). The cells were then washed with HBSS (+) to remove excess samples and observed by confocal microscopy. The cells were illuminated with a 488 nm laser to detect the localization of **RA** in the cell. Mitotracker deep red was illuminated with a 636 nm laser, and images were collected. For the spatial-selective photoexcitation, a 488 nm laser was used with time-lapse imaging.

Mander's colocalization coefficient. The Mander's colocalization coefficient for RA was obtained from the images shown in Figure 7A-C using ImageJ FiJi's plug-in Coloc 2.[4] The scatterplot to obtain the value is shown in Figure S12.

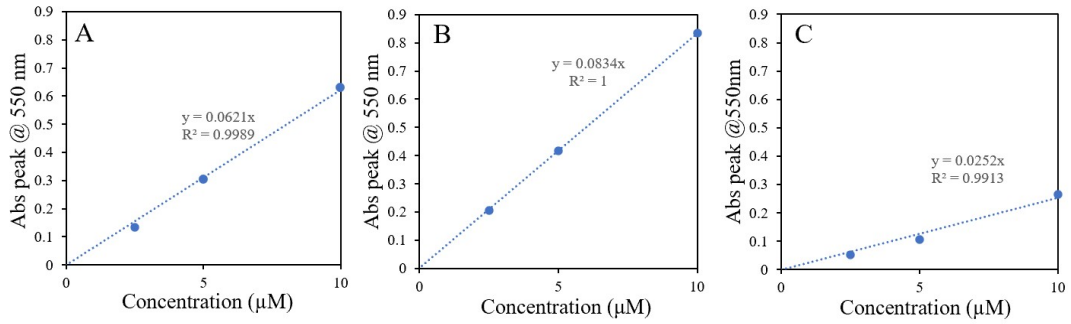

Figure S1. Plots of the absorbances of **RA** at 550 nm in (A) ethanol, (B) PBS, and (C) DMF, with concentrations of 2.5, 5.0, and 10 μM, corresponding with Figure 1.

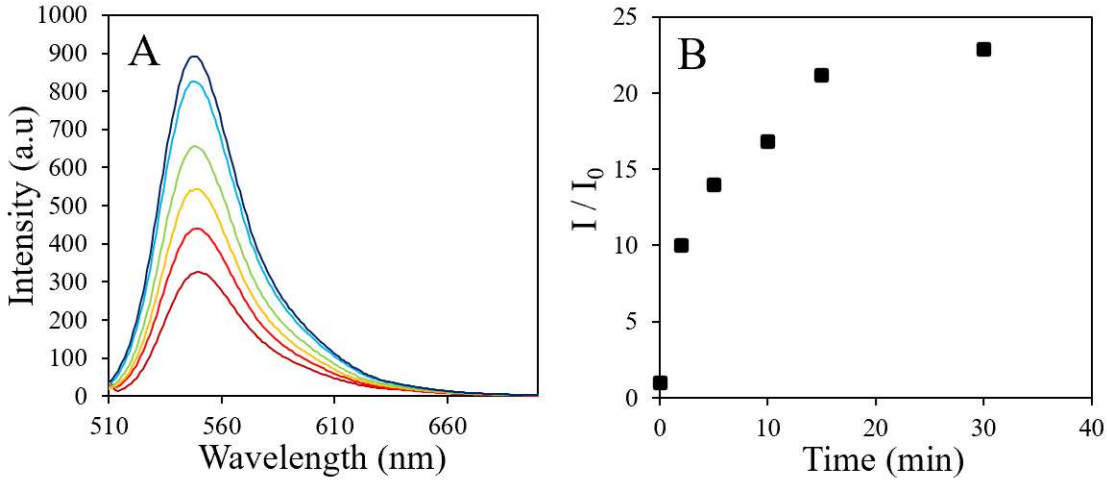

Figure S2. (A) Fluorescence spectra (λ_{ex}: 500 nm) of **RA** (2.5 μM) and TCPP (1.0 μM) in PBS with the 430 nm photosensitization for 30 min (red to blue lines), and (B) the corresponding time-trace of the relative fluorescence intensities at 560 nm.

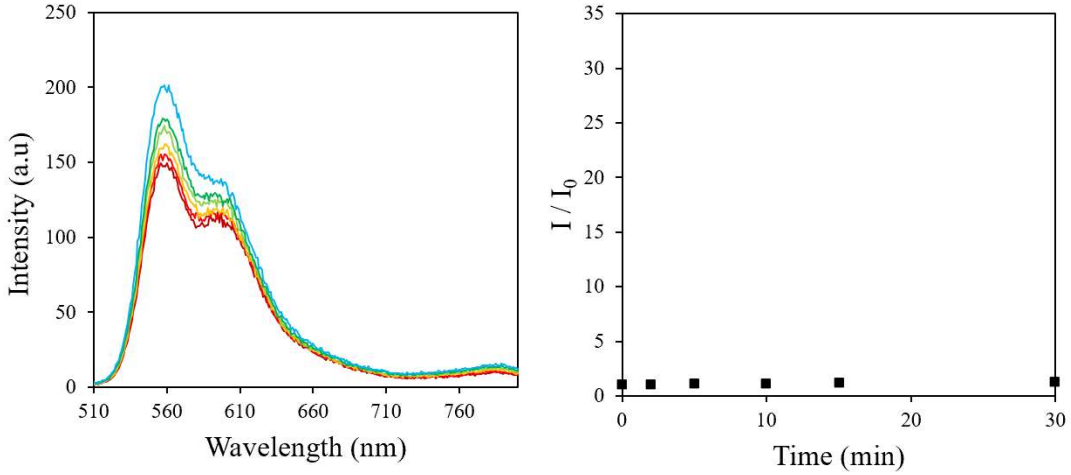

Figure S3 Fluorescence spectra (λ_{ex}: 500 nm) of **RA** (5.0 μM) in the absence of any photosensitizer in DMF before and after the 430 nm photoactivation (red to blue lines)

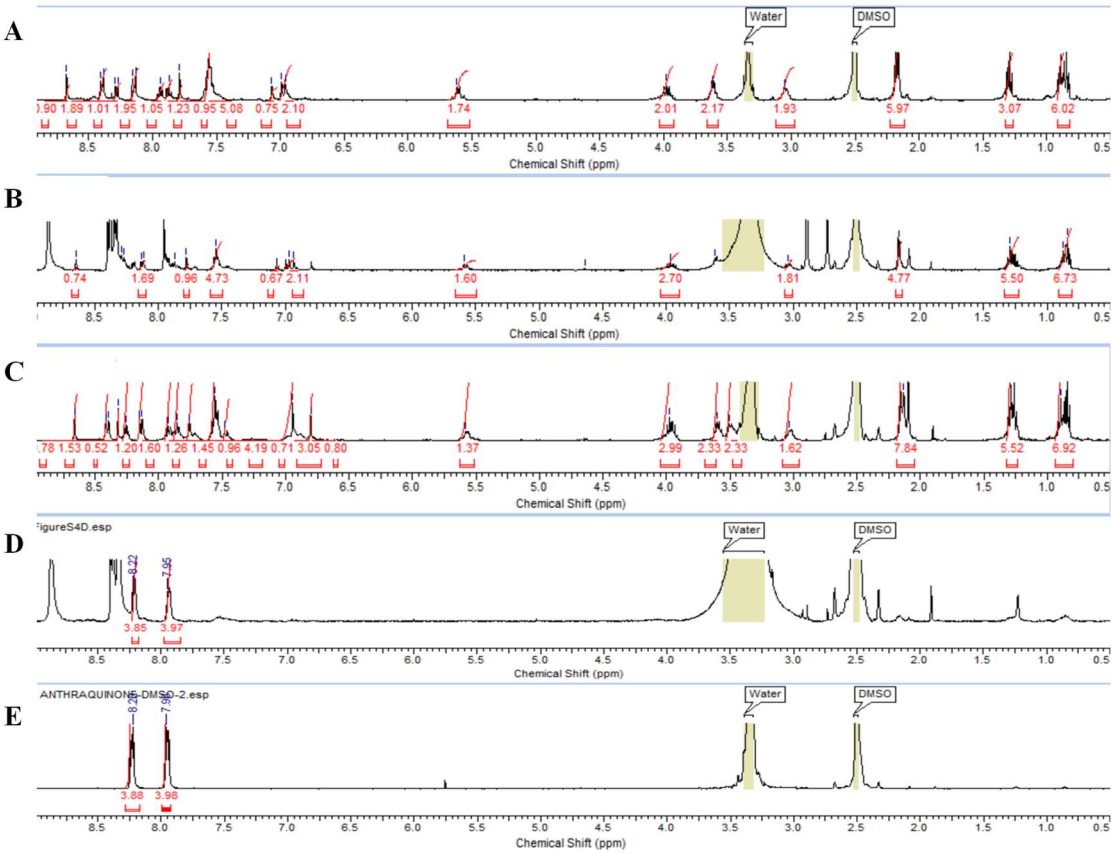

Figure S4. ^{1}H-NMR spectra of the mixed solution of 3.0 mM **RA** and 3.0 mM TCPP in DMF-d_7 (**A**) before and (**B**) after the illumination by 430 nm LED light (100 mW cm^{-2}), (**C** and **D**) the obtained two fractions after the separation by HPLC (5% $CHCl_3$-MeOH as the eluent), and (**E**) standard sample of quinodimethane. The fraction shown in (**D**) clearly demonstrates the signals from quinodimethane, which is shown in (**E**).

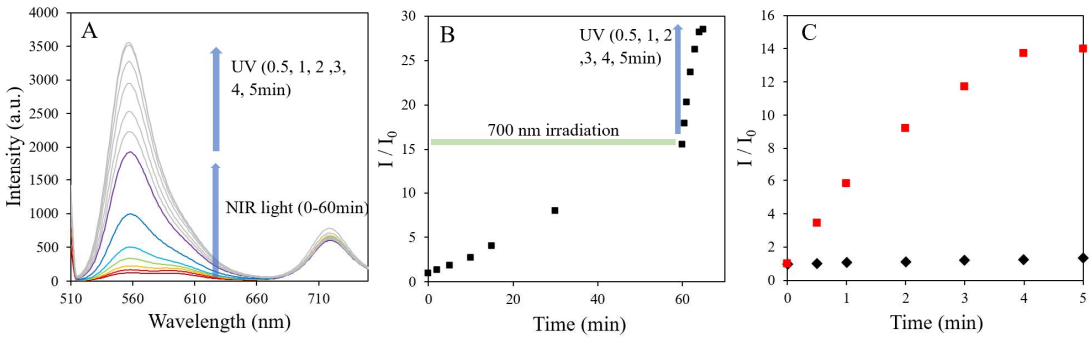

Figure S5. (A) Fluorescence spectra (λ_{ex}: 500 nm) of **RA** (10 μM) and rTPA (12.5 μM) in DMF before and after of the 700 nm photosensitization for 60 min (red to purple lines), followed by the photoactivation by the UV illumination (365 nm, 1.0 mW cm^{-2}) (grey lines), and (B) the corresponding time-traced relative fluorescence intensities at 560 nm. (C) Time-traced relative fluorescence intensities (at λ=560 nm) of **RA** with rTPA (red plots) with the primary 700 nm photosensitization and then the following UV photoactivation (365 nm, 1.0 mW cm-2), and (black plots) only with the UV photoactivation.

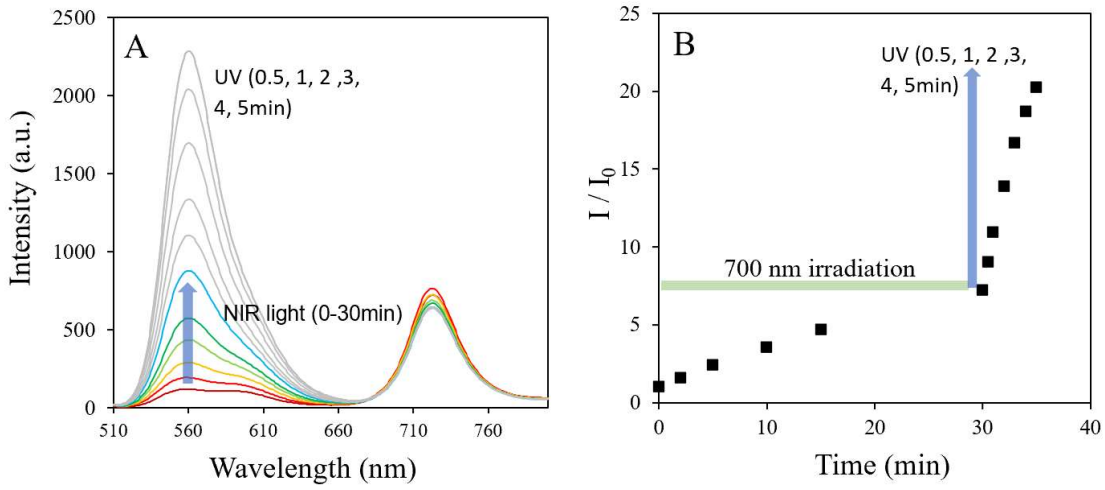

Figure S6 (A) Fluorescence spectra (λ_{ex}: 500 nm) of **RA** (10 μM) and rTPA (12.5 μM) in DMF before and after of the 700 nm photosensitization for 30 min (red to purple lines), followed by the photoactivation by the UV illumination (365 nm, 1.0 mW cm^{-2}) (grey lines), and (B) corresponding time-traced relative fluorescence intensities at 560 nm.

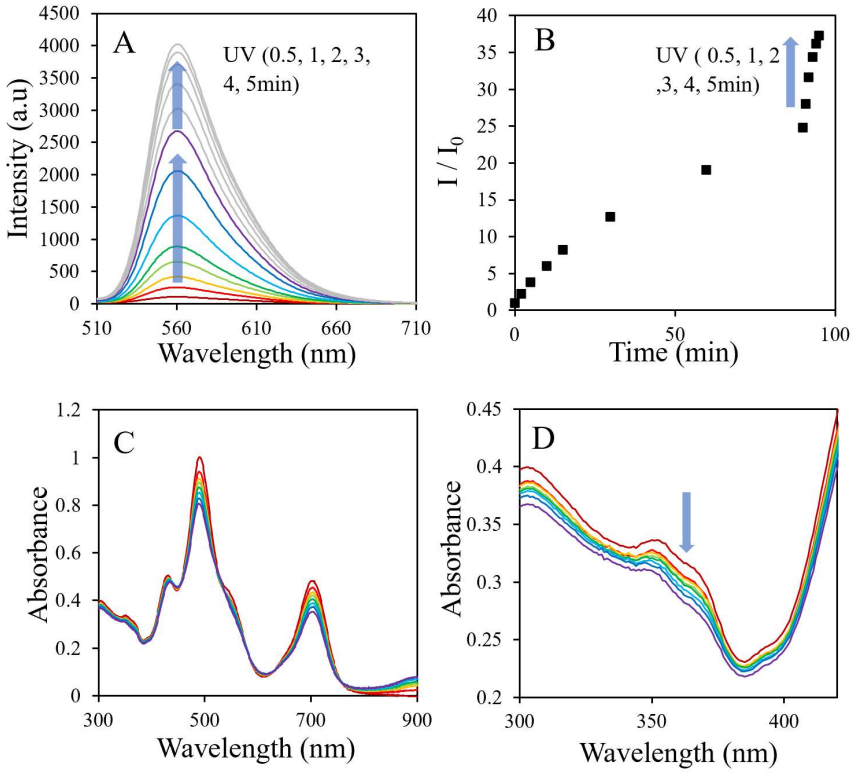

Figure S7. (A) Fluorescence spectra (λ_{ex}: 500 nm) of **RA** (10.0 μM) and **rTPA** (12.5 μM) in PBS before and after of the 700 nm photosensitization for 90 min (red to purple lines), followed by the photoactivation by the UV illumination (365 nm, 1.0 mW cm^{-2}) (grey lines), and (B) corresponding time-traced relative fluorescence intensities (at λ=560 nm). (C) Absorption spectra of **RA** (10.0 μM) and **rTPA** (12.5 μM) in PBS before and after the 700 nm photosensitization for 90 min (red to purple lines), and (D) its expanded spectra.

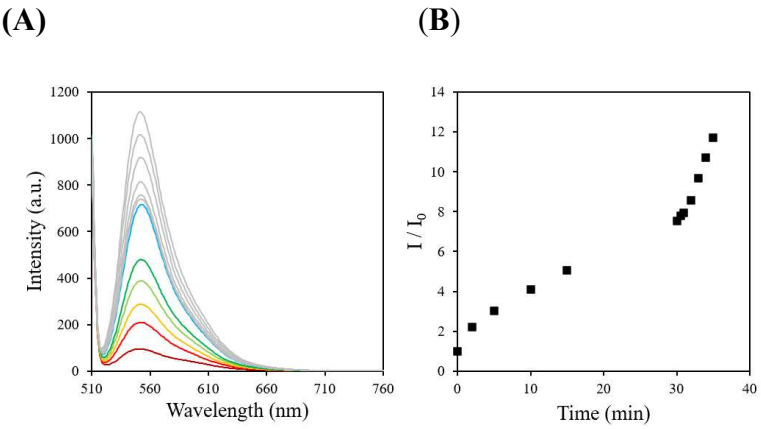

Figure S8. (A) Fluorescence spectra (λ_{ex}: 500 nm) of **RA** (10.0 μM) and **rTPA** (12.5 μM) in PBS before and after of the 700 nm photosensitizations for 30 min (red to blue lines), followed by the photoactivation by the green light illumination (530 nm, 1.0 mW cm^{-2}) (grey lines), and (B) corresponding time-traced relative fluorescence intensities at 560 nm.

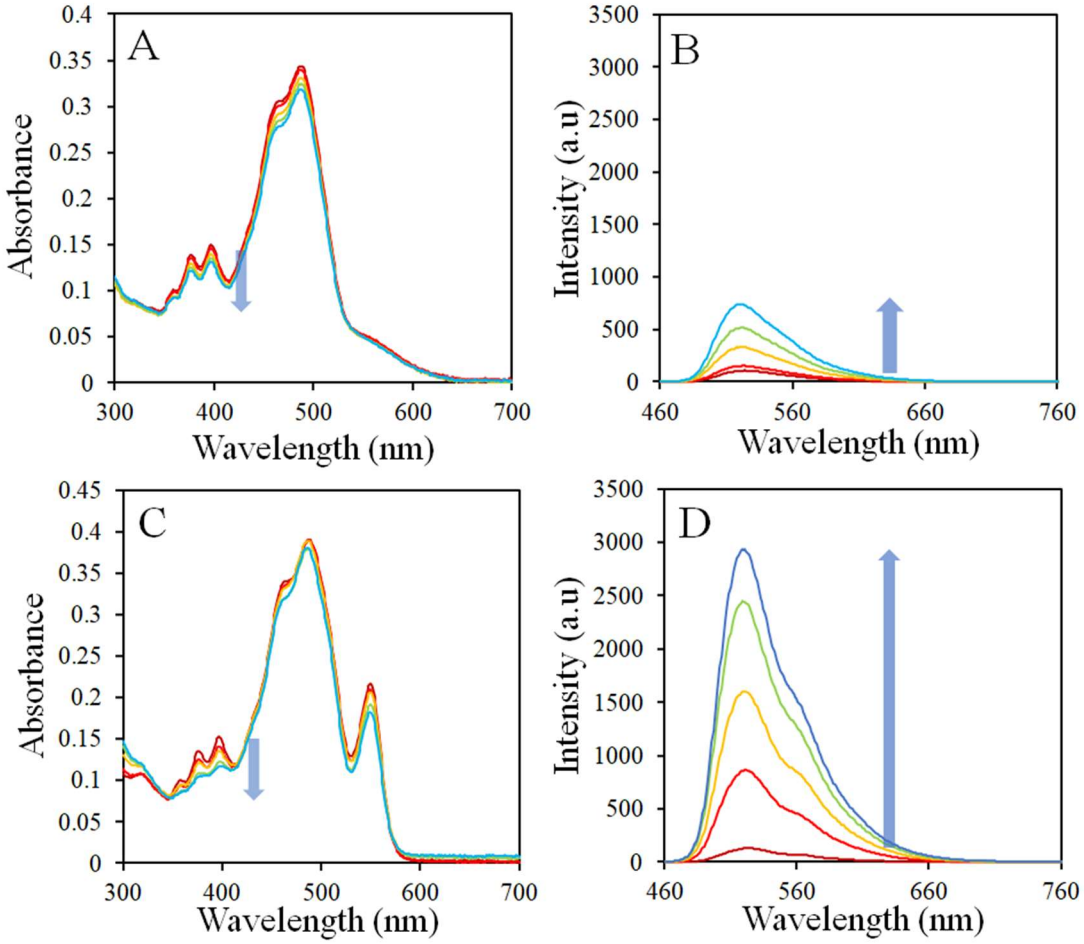

Figure S9. SOSG assays using 10 μM SOSG in 10mM HEPES aq. **(A)** Absorption spectra and (**B**) fluorescence spectra of 2.0 μM **RA** with SOSG, irradiated by a 532 nm green laser light (20 mW) for a photosensitized generation of $^1O_2$. **(C)** Absorption spectra and (**D**) fluorescence spectra of 2 μM rose bengal with SOSG, irradiated by a 532 nm green laser light (20 mW) for a photosensitized generation of $^1O_2$. The time intervals are 0, 2, 5, 10, 15, and 30 min.

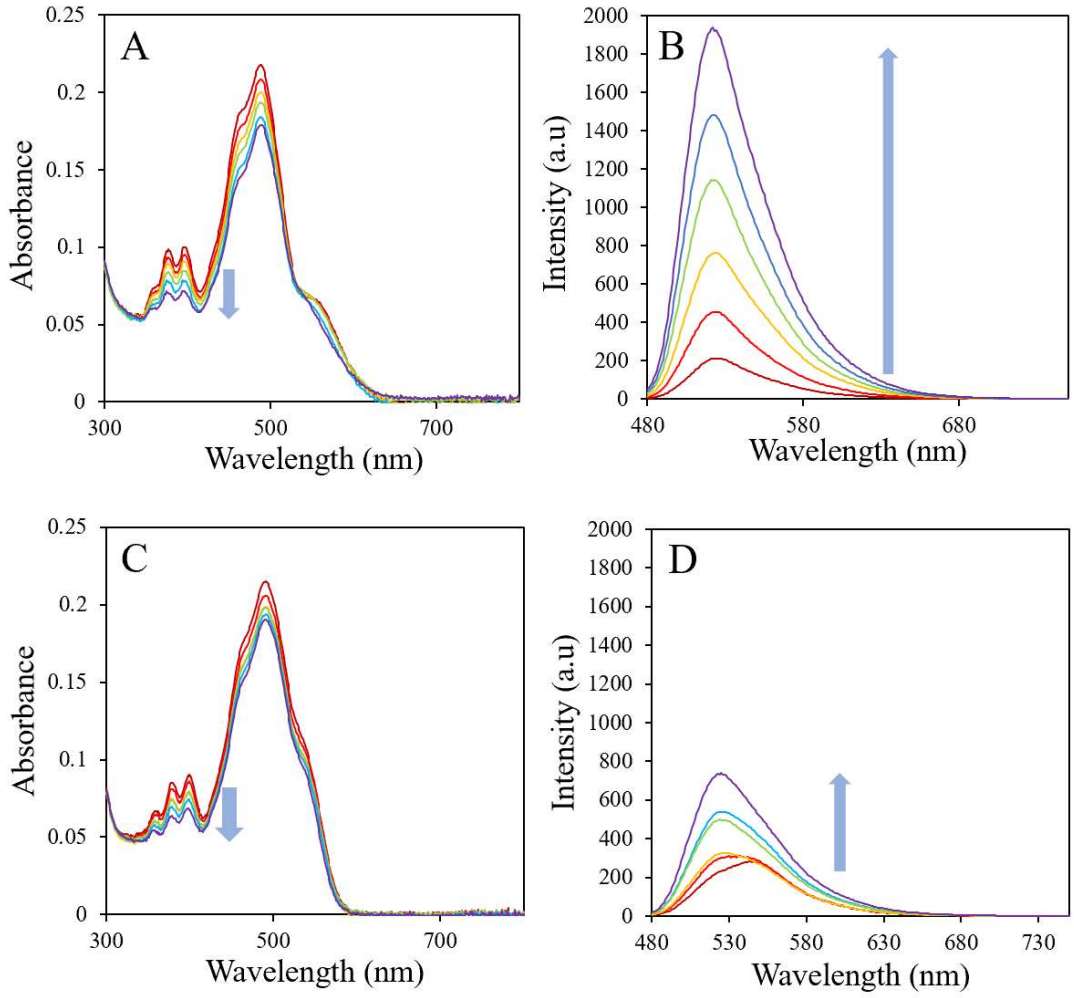

Figure S10. SOSG assays using 10 μM SOSG in 10mM HEPES aq. **(A)** Absorption spectra and (**B**) fluorescence spectra of 2.0 μM **RA** with SOSG, irradiated by a 560 nm light (20 mW cm^{-2}) for a photosensitized generation of $^1O_2$. **(C)** Absorption spectra and (**D**) fluorescence spectra of 2 μM rhodamine 6G with SOSG, irradiated by a 560 nm light (20 mW cm^{-2}) for a photosensitized generation of $^1O_2$. The time intervals are 0, 2, 5, 10, 15, and 30 min

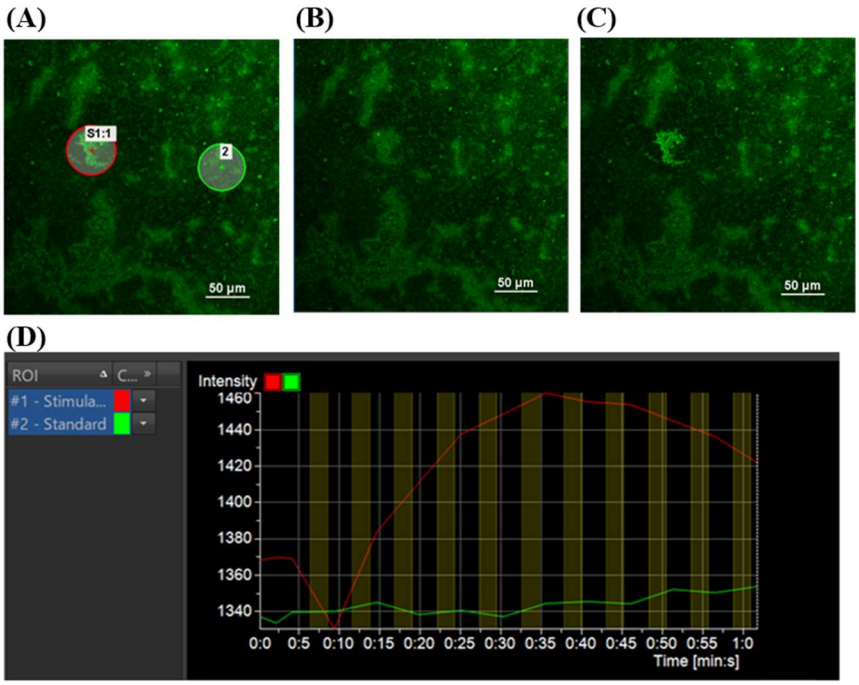

Figure S11. Spatioselective photoactivation of **RA** in lipid film. (A) The image showing the excited area by an intense 488nm laser (red circle) and the reference area without the laser excitation (green circle). Fluorescence images of (B) before and (C) after the 488nm excitation. (D) Fluorescence intensity plots of the red and green circle ROIs.

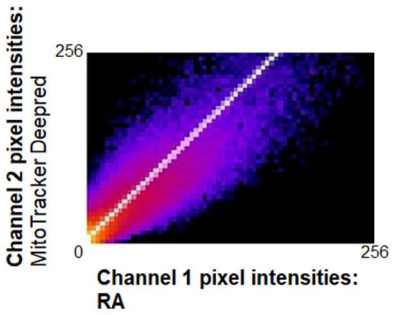

Figure S12. Scatterplot of green (channel 1: **RA**) and red (channel 2: MitoTracker Deep Red) pixels corresponding to Figures 7A-C to calculate the Mander's colocalization coefficient for **RA**.

References

[1] Satrialdi, R. Munechika, V. Biju, Y. Takano, H. Harashima, Y. Yamada, *Chem. Commun.* **2020**, *56*, 1145–1148.

[2] I. F. A. Mariz, S. N. Pinto, A. M. Santiago, J. M. G. Martinho, J. Recio, J. J. Vaquero, A. M. Cuadro, E. Maçôas, *Commun. Chem.*. **2021**, *4*, 142.

[3] T. Kishimoto, H. Ishikura, C. Kimura, T. Takahashi, H. Kato, T. Yoshiki, *In.. J. Cancer* **1996**, *69*, 290–294.

[4] J. Schindelin, I. Arganda-Carreras, E. Frise, V. Kaynig, M. Longair, T. Pietzsch, S. Preibisch, C. Rueden, S. Saalfeld, B. Schmid, J. Y. Tinevez, D. J. White, V. Hartenstein, K. Eliceiri, P. Tomancak, A. Cardona, *Nat. Methods* **2012**, *9*, 676–682.